Soil moisture and plant stress dynamics along the Kalahari precipitation gradient

Amilcare Porporato, Francesco Laio, and Luca Ridolfi
Dipartimento di Idraulica Trasporti ed Infrastrutture Civili, Politecnico di Torino, Torino, Italy

Kelly K. Caylor
Department of Environmental Sciences, University of Virginia, Charlottesville, Virginia, USA

Ignacio Rodriguez-Iturbe
Department of Civil and Environmental Engineering and Center for Energy and Environmental Studies, Princeton University, Princeton, New Jersey, USA

Received 15 April 2002; revised 28 August 2002; accepted 8 September 2002; published 14 February 2003.

[1] We present an analysis of water balance and plant water stress along the Kalahari precipitation gradient using a probabilistic model of soil moisture. The rainfall statistical characteristics, obtained from daily data of four stations along the transect, show that the rainfall gradient (from 950 to 300 mm/year) is mostly due to a decrease in the mean rate of storm arrivals (from 0.38 to 0.09 1/day) rather than to a change in the mean storm depth (practically constant at 10 mm). Using this information and typical vegetation and soil parameters, the analysis relates the vegetation properties along the transect with those of climate and soil. It is shown that differences in water balance and plant water stress between trees and grasses generate varying preferences for vegetation types along the transect, with deeper-rooted trees favored in the more mesic regions of the northern Kalahari and grasses favored in the drier zones of the southern Kalahari. The point of equal plant water stress is found at about 420 mm of rainfall during the growing season (October–April), indicating the possibility of tree-grass coexistence in the central sector of the Kalahari. These findings are consistent with patterns of vegetation distribution across the Kalahari transect. *INDEX TERMS:* 1866 Hydrology: Soil moisture; 1851 Hydrology: Plant ecology; 1836 Hydrology: Hydrologic budget (1655); 1818 Hydrology: Evapotranspiration; 1655 Global Change: Water cycles (1836); *KEYWORDS:* soil moisture dynamics, water balance, Kalahari, plant water stress, stochastic processes, ecohydrology

Citation: Porporato, A., F. Laio, L. Ridolfi, K. K. Caylor, and I. Rodriguez-Iturbe, Soil moisture and plant stress dynamics along the Kalahari precipitation gradient, *J. Geophys. Res.*, *108*(D3), 4127, doi:10.1029/2002JD002448, 2003.

1. Introduction

[2] The Kalahari sand sheet in Southern Africa is a 2.5 million km^2 area with relatively similar soil but a strong south-to-north increase in rainfall that provides an excellent basis for gradient studies at subcontinental scale. For this reason the International Geosphere-Biosphere Programme has designated the Kalahari Transect as one of its "mega-transects" to explore continental-scale links between climate, biogeochemistry, and ecosystem structure and function [*Scholes and Parsons*, 1997; *Scholes et al.*, 2002; *Swap et al.*, 2001; *Dowty et al.*, 2001; *Annegarn et al.*, 2001].

[3] This paper focuses on water balance and plant water stress along the Kalahari transect. After a general introduction to the climate and vegetation of the region, the rainfall stochastic structure in some stations along the transect is studied. The soil moisture dynamics and plant stress are then analyzed, using the probabilistic model recently proposed in a series of papers by *Rodriguez-Iturbe et al.* [1999a], *Laio et al.* [2001a], and *Porporato et al.* [2001].

0148-0227/03/2002JD002448$09.00

1.1. Climate

[4] Variations in rainfall are much more important than temperature in the Kalahari environment. Kalahari climate ranges from the aridity of southwestern Botswana to the humid tropical conditions of western Zambia and eastern Angola. The latitudinal spread and the main features of regional atmospheric circulation combine to establish a south-to-north gradient of increasing mean annual rainfall as seen in Figure 1 [*Tyson*, 1986; *Tyson and Crimp*, 1998]. On average, over 80% of the annual rainfall occurs between October and April. Only in the extreme northern and southern portions of the Kalahari sands is seasonality reduced, due to the yearlong dominance of equatorial convection in the north, and the effect of winter South Atlantic cyclones in the south. Besides the seasonal patterns of precipitation, marked interannual variations are also present. Likewise, the onset and duration of the growing season (wet season) vary considerably from year to year: as

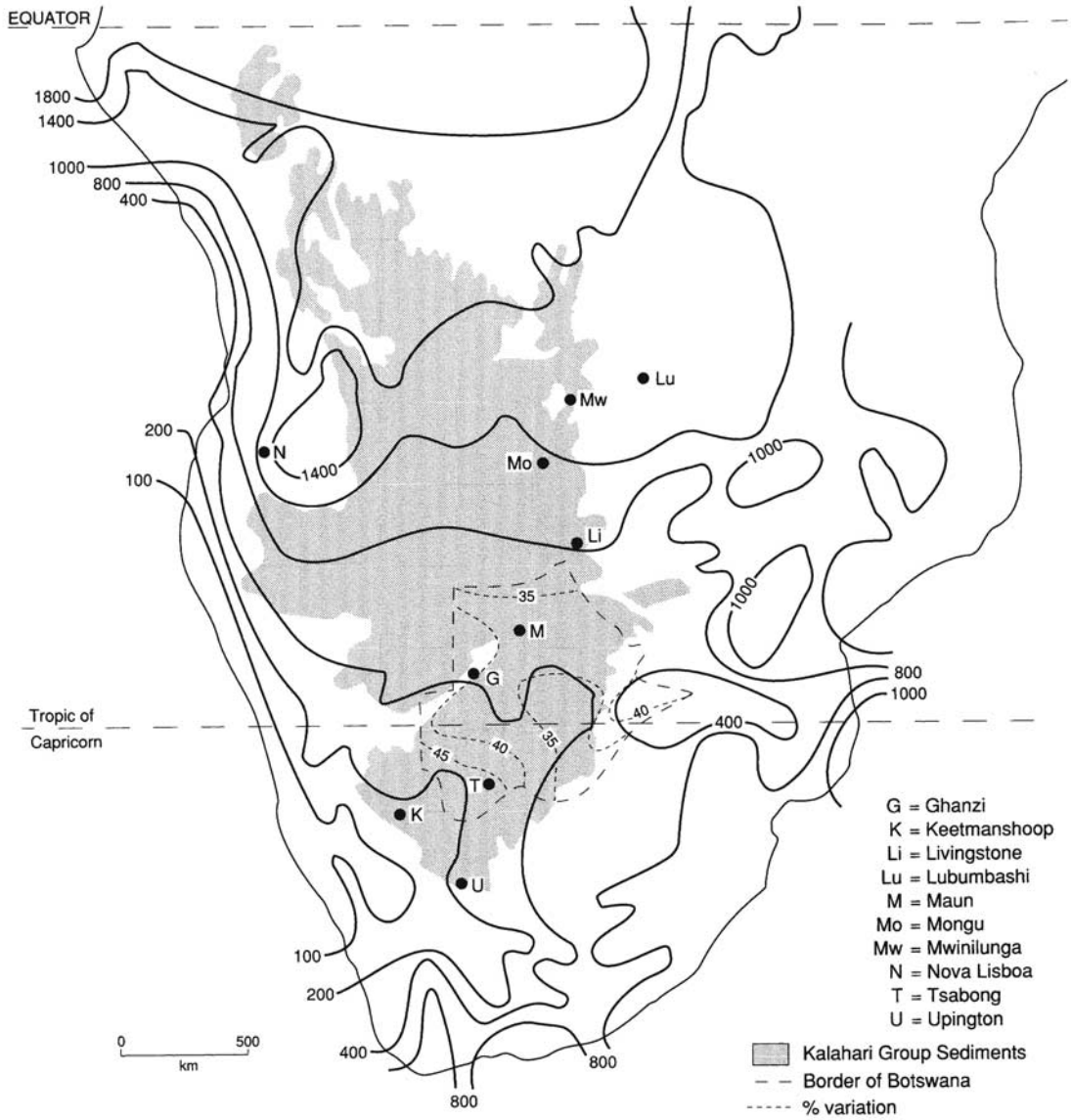

Figure 1. Mean annual rainfall (mm) over Southern Africa and annual CV over Botswana, after *Thomas and Shaw* [1991].

the length of the wet season and total precipitation amounts decrease in the south and westerly direction, so the inter-annual variability increases. As shown in Figure 1, the annual coefficient of variation of rainfall exceeds 45% in the driest areas of the southwestern Kalahari.

[5] Most of the rain is in the form of convective thunderstorms, which tend to occur in the late afternoon and early evening. As noticed by *Thomas and Shaw* [1991], however, while most rainfall is derived from high-intensity showers, not every event is a significant one. This is an important aspect for plant water availability, and we will return later to this point when discussing the statistics of the daily amounts of rainfall.

1.2. Soil and Vegetation

[6] The soils of the Kalahari are relatively homogenous, mainly made up of sandy sediments. The very low content of organic materials and nutrients makes Kalahari soils highly infertile and places plants under extreme conditions of water and nutrient deficit. This effect is especially strong in the southwestern Kalahari, where low rainfall, reduced atmospheric humidity, and high temperatures increase plant stress.

[7] The distribution of vegetation essentially follows the gradient in precipitation and soil moisture. Here we will mostly refer to the vegetation of the Kalahari sandveld, i.e., the one on deep, well-drained sand, neglecting other geomorphologically related ecosystems of local character, such as inter-dune hollows, pan and lake basins, drainage lines, and riverine and swamps habitats, in which the Kalahari is also abundant [*Thomas and Shaw*, 1991].

[8] The vegetation type on the sandveld can be broadly defined as a savanna, in the sense of a transition between tropical forest and open grassland [*Thomas and Shaw*, 1991; *Scholes et al.*, 2002]. Schematically, going from the most

xeric to the most mesic regions, the so-called Kalahari desert of the southern part of the transect largely consists of desert grasslands dominated by annuals and only sporadically interrupted by shrubs and few trees. Moving north, trees and shrubs begin to occur in thickets until the deep, soft sands and greater amounts of rainfall in the northeastern Kalahari often allow trees to develop more abundantly, forming either moist savanna or dry deciduous woodlands [*Thomas and Shaw*, 1991].

[9] From a quantitative viewpoint, the vegetation types form a relatively orderly progression of increasing woody plant cover and height with rainfall gradient. *Scholes et al.* [2002] report the results of an investigation of 10 sites from Zambia to South Africa and show that the overall trend is for the woody biomass, basal area, cover, and height to increase with increasing availability of water to the plants. The increase in woody cover is also associated with an increase in woody plant diversity as well as with a decrease in the relative importance of grasses as contributors of the site biomass. In particular, the absolute grass biomass increases with increasing rainfall up to about 600 mm, and then decreases due to competition from woody plants at higher rainfall levels.

2. Methods

2.1. Rainfall Data

[10] The first step in our analysis is the statistical examination of the historic record of daily rainfall data for a set of stations distributed along the Kalahari transect. Our main goal is to assess the seasonal patterns and the statistical characteristics of the rainfall regime (e.g., mean frequency and mean depth of rainfall events), since these factors control the onset and duration of the growing season as well as the soil moisture availability for plant growth and plant water stress.

[11] Four stations, i.e., Mongu, Sesheke, Senanga, and Vastrap, are considered. The first three are along the Zambezi River in western Zambia, in a region placed between the 15° S and the 18° S parallel, which is in the northern part of the transect. The fourth, Vastrap, is located in the southern part of the transect close to the 28° S parallel. Unfortunately, other stations more homogeneously distributed along the transect had to be excluded, either because of the small number of years of observation or because of the too many gaps present in the record.

2.2. Soil Moisture Model

[12] Using the rainfall data, the probabilistic soil moisture dynamics may be studied following the approach by *Rodriguez-Iturbe et al.* [1999a] and *Laio et al.* [2001a]. The starting point of the model is the stochastic differential equation for the soil water balance, i.e.,

$$nZ_r \frac{ds}{dt} = I(s,t) - E(s) - L(s), \tag{1}$$

where n is the porosity, Z_r is the active depth of soil, s is the relative soil moisture content, $I(s, t)$ is the rate of infiltration from rainfall, $E(s)$ is the rate of evapotranspiration, and $L(s)$ is the rate of leakage or deep infiltration.

[13] Rainfall is stochastically represented as a Poisson process of storm arrivals in time with rate λ, each storm having a depth h, modeled as an exponentially distributed random variable with mean α. Rainfall results in an infiltration depth into the soil, $I(s, t)$, which is taken to be the minimum of h and $nZ_r(1\text{-}s)$ to reflect the fact that only a fraction of h can infiltrate when the rainfall amount exceeds the storage capacity of the soil column. Excess rainfall produces runoff according to the mechanism of saturation from below [*Dunne*, 1978]. Canopy interception is included in the model by assuming a threshold of rainfall depth, Δ, below which no water effectively penetrates the canopy. All model results are interpreted at the daily timescale [*Rodriguez-Iturbe et al.*, 1999a; *Laio et al.*, 2001a].

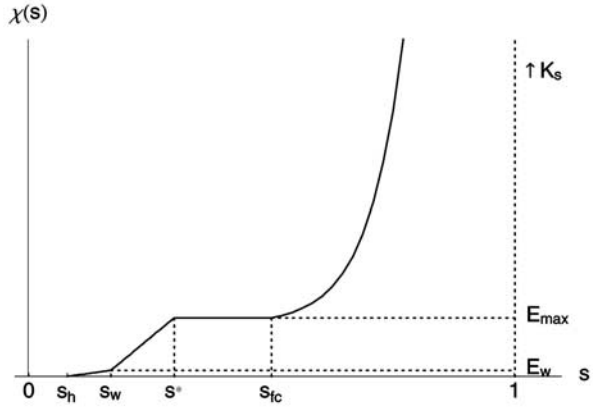

Figure 2. Behavior of soil water losses (evapotranspiration and leakage), $\chi(s)$, as function of relative soil moisture for typical climate, soil, and vegetation characteristics in semiarid ecosystems.

[14] The term $E(s)$ incorporates losses due to evaporation from the soil and transpiration from the plant. At the daily timescale it may span three regimes. Regime 1, or soil evaporation regime, defines $E(s)$ as linearly increasing with s from 0 at the hygroscopic point, s_h, to, E_w, at the wilting point, s_w. Regime 2, or stressed evapotranspiration regime, has a linear rise in $E(s)$ from E_w at s_w to E_{max} at s^*, where s^* is the soil moisture level at which the plant begins to close stomata in response to water stress and E_{max} is the climate and vegetation dependent maximum daily evapotranspiration rate. Regime 3 is the unstressed evapotranspiration regime, where evapotranspiration is decoupled from soil moisture and remains constant at E_{max}, which represents the average daily evapotranspiration rate during the growing season under well watered conditions.

[15] Assuming no interaction with the underlying soil layers and water table, $L(s)$ represents vertical percolation with unit gradient

$$L(s) = \frac{K_s}{e^{\beta(1-s_{fc})} - 1}\left[e^{\beta(1-s_{fc})} - 1\right], \tag{2}$$

where K_s is the saturated hydraulic conductivity, s_{fc} is the field capacity, and $\beta = 2b + 4$ with b the pore size distribution index. The sum of the evapotranspiration and leakage losses is shown in Figure 2. The values of s_h, s_w, s^*, and s_{fc} are related to the corresponding soil matric potentials through the empirically determined soil-water retention curves [*Clapp and Hornberger*, 1978]; s_w and s^* also depend on the vegetation type [*Laio et al.*, 2001a].

[16] The analytical expression for the steady state probability density function (pdf) of soil moisture as well as the

Table 1. Rainfall Characteristics for the Stations Considered Along the Kalahari Transect

Station	Observation Period[a]	R, mm/year	α, mm	λ, day^{-1}	CV_α	CV_λ	$\rho_{\alpha\lambda}$
Mongu	1935–92 (46)	942	10.1	0.38	0.17	0.16	0.01
Sesheke	1950–92 (39)	715	9.5	0.30	0.20	0.18	0.26
Senanga	1979–92 (14)	737	9.5	0.32	0.16	0.12	0.22
Vastrap	1973–96 (20)	305	10.3	0.09	0.31	0.32	0.21

[a]The number of years considered is given in parentheses.

expressions for the water balance components during the growing season are given by *Laio et al.* [2001a] under the assumption of statistically homogeneous growing season climate.

2.3. Plant Water Stress

[17] Starting from the probabilistic description of soil moisture dynamics, *Porporato et al.* [2001] developed the analytical tools characterizing the plant water stress in water-limited ecosystems. A first characterization of plant conditions is provided by the static vegetation water stress, ς, modeled by linking the actual soil moisture level to two soil moisture levels, s^* and s_w, associated with important changes in the physiological activities of the plant. Static stress is assumed to be equal to zero when soil moisture is above s^* and equal to 1 when soil moisture is at or below s_w. In between these soil moisture levels, the static stress is given by

$$\varsigma(t) = \left[\frac{s^* - s(t)}{s^* - s_w}\right]^q, \tag{3}$$

where q is a measure of the nonlinearity of the effects of soil moisture deficit on plant conditions. The mean value of water stress given that the plant is under stress, $\bar{\varsigma}'$, is calculated by only considering the part of the pdf corresponding to ς values greater than 0.

[18] Besides the information given by $\bar{\varsigma}'$, the dynamical aspects of the water deficit process, namely the duration and frequency of the stress periods, should also be taken into account to fully describe the plant stress conditions. To this purpose, *Porporato et al.* [2001] derived the expressions for the mean length, $\bar{T}_\xi$, of an excursion below an arbitrary soil moisture threshold, ξ, as well as the mean number, $\bar{n}_\xi$, of such intervals during the growing season. The two crucial thresholds to which these expressions have been explicitly applied are again s_w and s^*.

[19] The above information on the stress intensity, its mean duration, and its frequency of occurrence may be combined to define the dynamical water stress. This overall indicator of the condition of the plant under given edaphic and climatic factors is equal to

$$\bar{\vartheta} = \left(\frac{\bar{\varsigma}'\,\bar{T}_{s^*}}{kT_{seas}}\right)^{\frac{1}{\bar{n}_{s^*}}} \tag{4}$$

if $\bar{\varsigma}'\bar{T}_{s^*} < kT_{seas}$ and 1 otherwise. The parameter k is an indicator of plant resistance to water stress and T_{seas} is the duration of the growing season.

3. Results and Discussion

3.1. Precipitation Regime

[20] The main statistics relative to the rainfall data are reported in Table 1. The mean annual behavior of precipitation, shown in Figure 3, reveals a marked seasonality and similar annual regimes for Mongu, Sesheke, and Senanga. For these stations the dry period occurs between May and September, while the wet season goes from October to April; this latter period will be assumed to coincide with the growing season. The months of July and August are on average the driest ones: for all these stations no rainfall was recorded in July during the periods considered, while some occasional events occurred in September.

[21] The rainfall regime at Vastrap requires a separate discussion. As can be seen from Figure 3d, the seasonality is almost nonexistent, owing to sporadic winter rainfall associated with mid-latitude disturbances typical of the southernmost Kalahari regions. This anomalous behavior, also noticed by *Scholes et al.* [2002], will become even more apparent in the subsequent analysis of the statistics of the interstorm periods. It is clear that because of the low total annual precipitation and the lack of any recurrent behavior, Vastrap vegetation must rely on these occasional events randomly distributed along the year rather than on a regular (wet) growing season. Notwithstanding this fact, however, the same period form October to April will be chosen as a reference growing season for all four sites, for the sake of comparison among the stations.

[22] Figure 4a presents the relative frequency of rainfall depth, h, for rainy days during the growing season for each of the four stations. Both the mean value, α, (Table 1) and the trends (Figure 4a) are quite similar for all the stations, so that a value of α = 10 mm/event will be used in all the following analyzes for the probabilistic rainfall model. Notice also that the histograms follow an exponential distribution like the one assumed in the stochastic rainfall model driving the soil moisture dynamics.

[23] It is also apparent from Figure 4a that most events are of low intensities for all the stations. This is in agreement with the analysis of Botswana data by *Pike* [1971], where over 80% of rainfall events were found to be of low intensity and rainfall amounts were less than 10 mm for about half of the total number of events. These characteristics have very important implications for vegetation, since interception and surface evaporation may become dominant components of the water balance during such light rainfall events [*Porporato et al.*, 2001].

[24] The previous analysis implies that the decrease in the mean rainfall amount is mostly a consequence of a reduction in the rate of storm arrivals when moving from north to south. This is confirmed by the mean value of the rate of storm arrivals, λ, that dramatically decreases from more than one event every three days in Mongu to less than one event every eleven days in Vastrap in the period from October to April (Table 1). The relative frequency of the interstorm times, τ, are presented in Figure 4b. For Mongu, Sesheke, and Senanga, the distribution is well

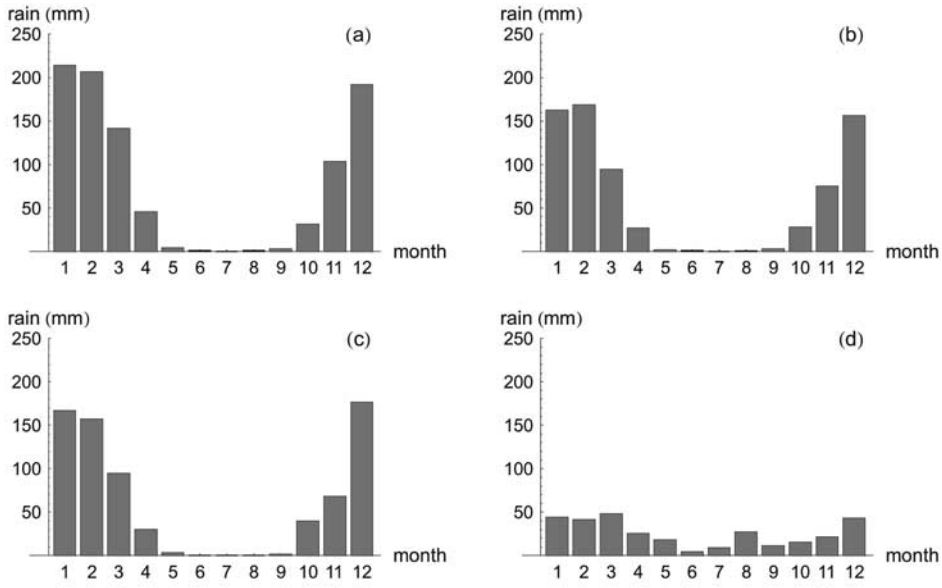

Figure 3. Seasonal variability of rainfall for the four stations considered: (a) Mongu, (b) Sesheke, (c) Senanga, and (d) Vastrap.

described by an exponential decay, thus agreeing with the Poisson model used for the rainfall arrivals. Only in Vastrap the distribution of arrival times is completely different, being almost uniform in the range 1–15 days. This confirms the peculiar rainfall regime of this southern pre-desertic site, characterized by single, sometimes intense events separated by long dry periods, which may last several weeks.

[25] Table 1 also shows the coefficients of variation for α and λ, which exhibit a marked inter-annual variation around the mean values for each site. No significant correlation, $\rho_{\alpha,\lambda}$, between these two rainfall parameters is present. The interannual variability appears to be particularly extreme for the mean rainfall depth, α, in Vastrap.

[26] The mean rainfall depth per event, α, is assumed to be spatially uniform and equal to 10 mm, while the mean rate of event arrivals, λ, is varied in the range between 0.5 and 0.1 d^{-1} going from north to south along the transect (Figure 5).

3.2. Soil Moisture and Plant Water Stress

[27] Since the soil type is uniformly sandy with a low content of soil organic matter, very low adhesion forces by the soil matrix exist which result in low soil moisture values at the hygroscopic point and at field capacity. These values are assumed to be $s_h = 0.04$ and $s_{fc} = 0.35$ respectively, while porosity, n, is assumed to be equal to 0.42.

[28] Table 2 gives an indication of likely values of the model vegetation parameters for some of the most common species in the Kalahari transect. From these data, it can be noticed that trees tend to have higher s_w and lower s^* than grasses. As in the case of the Nylsvley savanna [*Scholes and Walker*, 1993; *Laio et al.*, 2001b], this difference can be explained by the greater drought resistance and improved water use efficiency of C_4 grasses. In contrast to their improved water relations under drought conditions, grasses often have 10% higher maximum transpiration rates than tress in well-watered conditions (R. J. Scholes, personal communication, 1998). Mean typical values for trees will be assumed as $s_w = 0.06$, $s^* = 0.12$, and $E_{max} = 0.45$ cm/day, while for grasses $s_w = 0.05$, $s^* = 0.17$, and $E_{max} = 0.50$ cm/day will be used.

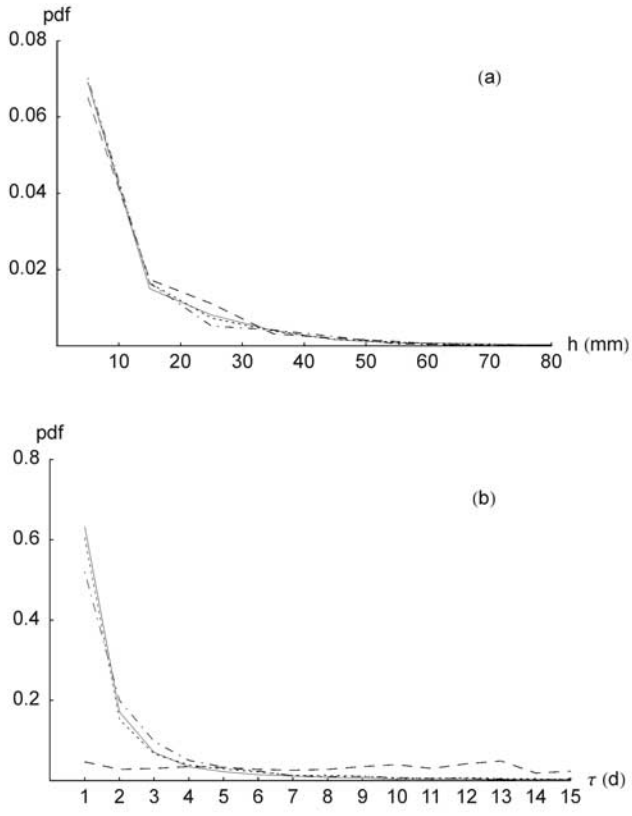

Figure 4. (a) Relative frequency of daily rainfall depth; (b) relative frequency of interstorm times. Mongu (continuous line), Sesheke (dotted line) Senanga (chain line) Vastrap (dashed line).

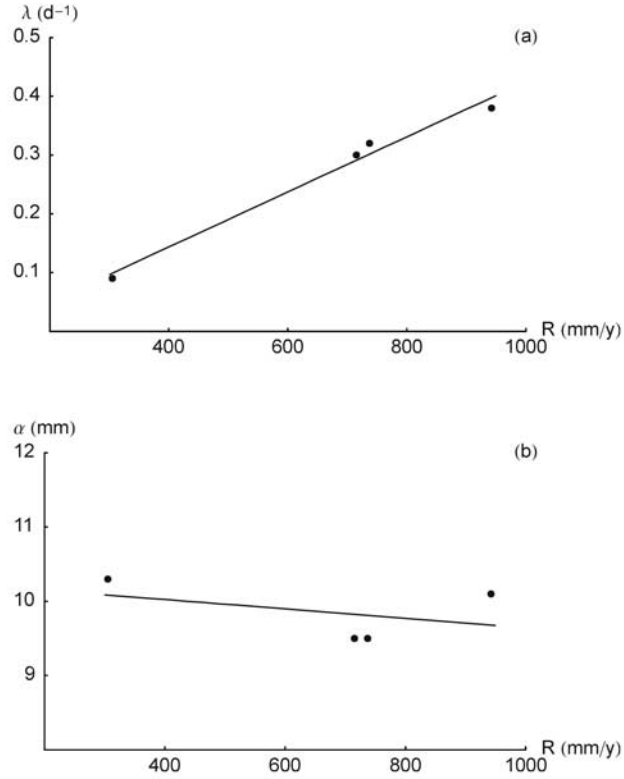

Figure 5. Mean frequency (a) and mean depth (b) of rainfall events as a function of mean annual rainfall, R.

[29] Although all the species are expected to root throughout the upper 1-meter of soil, grass roots are typically more concentrated closer to the soil surface, while the density of tree roots is more uniform throughout the profile. On account of this, the parameter Z_r (representing the effective rooting depth) is assumed as $Z_r = 100$ cm for tress and $Z_r = 40$ cm for grasses.

[30] Figure 6 displays the pdf of soil moisture for the case of trees as a function of λ over the range of values encountered along the transect. As λ increases, the shift of the pdf towards higher soil moisture values is evident, progressively moving out of the wilting region and into the region of nonstressed conditions. The variance of the distribution also increases with rainfall, mostly because in very arid climates the pdf is bounded from below by the wilting and the hygroscopic points. A similar computation for the grasses shows an analogous behavior but with higher variance. In the case of trees, the soil moisture attains very high or low values less frequently than grasses, supporting the results of *Laio et al.* [2001a] in their analysis of the general dependence of the soil moisture pdf as a function of Z_r.

[31] The computations of the long-term water balance show, as expected, that the water balance over the entire transect is dominated by losses due to evapotranspiration. As for the other main components of the balance, runoff is practically absent while leakage becomes nonnegligible only in the more humid northern regions for the case of shallow rooting depths. Interception can be quite important where the canopy cover is denser because of the relatively

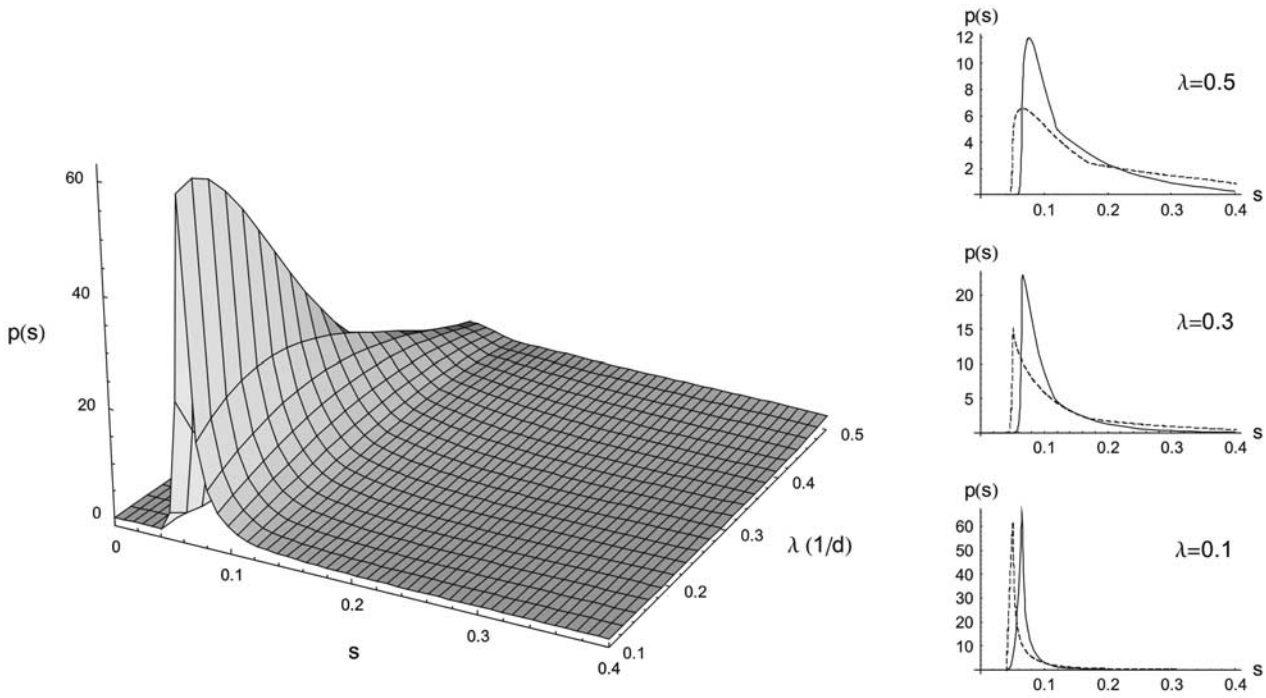

Figure 6. Soil moisture pdf as a function of λ for the range of values encountered along the Kalahari transect and using the mean parameter values of trees. The three examples in the insets have mean rainfall rates that are typical of the northern, central, and southern Kalahari, respectively (trees: continuous line; grasses: dashed line).

Table 2. Vegetation Characteristics for the Most Common Plants in the Zone of the Transect Analyzed by *Scholes et al.* [2002][a]

Species	s_w	$\Psi_{s,w}$(MPa)	s^*	Z_r(cm)	E_{max}(cm/d)
Erythrophleum africanum	0.060	−3.0	0.12	100	0.45
Ochna pulchra	0.060	−3.1	0.14	100	0.39
Pterocarpus angolensis	0.060	−3.0	0.12	100	0.45
Digitaria spp	0.061	−2.9	0.22	40–60	0.47
Eragostris spp	0.052	−3.9	0.15	40–60	0.61
Brachiaria nigropedata	0.058	−3.2	0.16	40–60	0.50

[a]Data from *Scholes and Walker* [1993] and other sources.

high fraction of events of low intensity (Figure 4a). The interception parameters used here are $\Delta_t = 2$ mm for tress and $\Delta_g = 1$ mm for grasses.

[32] Figure 7 presents the evapotranspiration and leakage components of the water balance computed as a function of the plant rooting depth Z_r and the rate of storm arrivals, λ, using the mean typical values of the evapotranspiration function for grasses and a fixed $\alpha = 10$ mm/event. From Figure 7a it is seen that the percentage of unstressed evapotranspiration can be maximized by adjusting the plant rooting depth. Thus, going from arid to humid climates, the best exploitation of the available soil water is achieved by increasing Z_r. As a consequence, with their 40–60 cm effective rooting depth, grasses are favored in the drier regions, while in the more humid regions the situation is reversed. This is due to more effective water use and decreased leakage losses provided by the different rooting depths. As Figure 7b shows, if the rooting depth does not extend below 70 cm, leakage losses may become non-negligible for wet sites, whereas for dry sites the existence of roots below 40–60 cm makes almost no difference. Thus, in the northern regions, deeper roots are important to extract water that otherwise would percolate below the rooting depth, while in the driest regions, where competition is mostly against evaporative losses, the effort of growing deeper roots becomes pointless in the absence of a permanent source of deep subsurface water. It is essential to stress that, both because the model only considers different values of rooting depth without modeling the soil moisture profile and because of the uncertainties in some of the parameter values, the results presented here are not intended to provide quantitative predictions, but should be interpreted as indicative of the relative importance of the various physical processes acting in the soil-plant system along the transect.

[33] The role of the rooting depth on overall plant conditions as well as that of the competition between plant transpiration and the other soil water losses become more evident when considering the intensity and the temporal statistics of the periods of plant stress (e.g., dynamical water stress, Equation (4)).

[34] Figure 8 shows the dynamical water stress computed as a function of the rate of event arrivals for the mean parameter values representative of trees and grasses. As expected, the general behavior is one of progressive increase of plant stress going from wet to dry climates. The plateau for intermediate values of λ is a consequence of

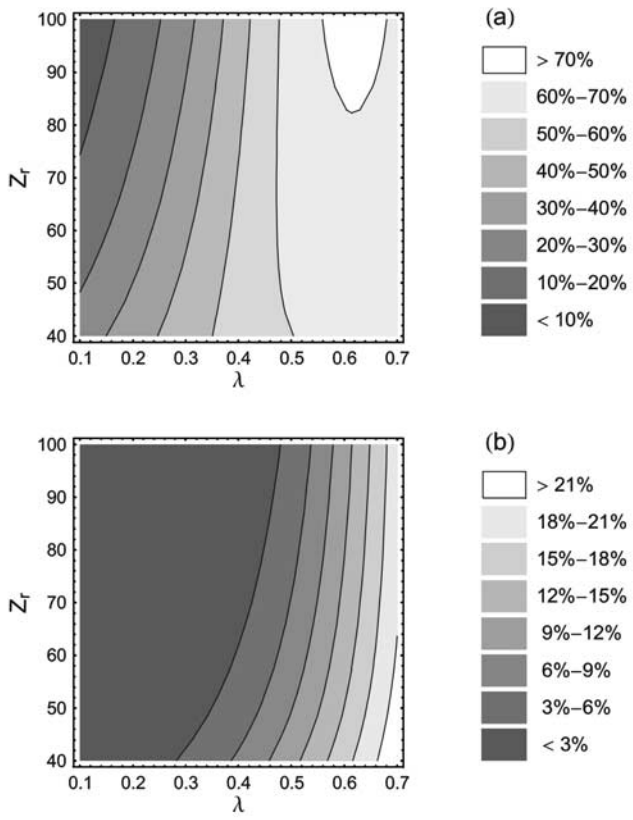

Figure 7. Soil water balance using the mean typical transpiration function for grasses. (a) Percentage of unstressed evapotranspiration as a function of λ and Z_r. (b) Percentage of leakage losses as a function of λ and Z_r.

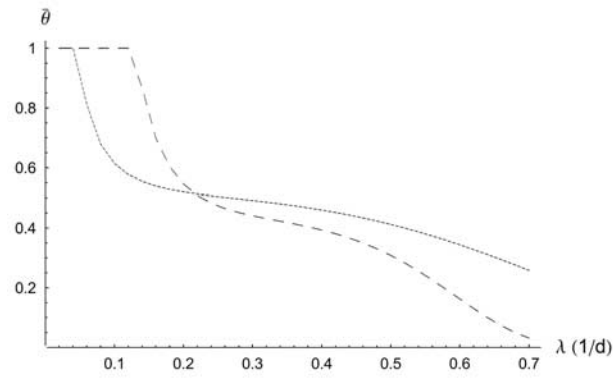

Figure 8. Behavior of the dynamical water stress as a function of the mean rainfall rate for trees (dashed line) and grasses (dotted line). $\alpha = 1$ cm, $T_{seas} = 210$ d; see text for the values of the other parameters.

the interplay between the frequency of periods of water stress, which attains its maximum in such a zone, and the duration of the stress periods, which increases with decreasing λ [*Porporato et al.*, 2001]. The dependence of the dynamic stress on λ is more marked for trees than for grasses. In particular, grasses are able to maintain relatively low stress levels even at very low rainfall rates. This is partially due to their lower wilting point, which reduces the effect of water deficit on the plant. More importantly, grasses benefit from their shallow rooting depth, which allows increased access to light rainfall events and reduces the occurrence of long periods of water stress [*Porporato et al.*, 2001; *Laio et al.*, 2001b].

[35] The point of equal stress, which could be interpreted as identifying a region of tree-grass coexistence, is found at $\lambda = 0.2\ d^{-1}$, which corresponds to a total rainfall of approximately 420 mm for the 7-month period of the wet season (October to April). The fact that the slope of the two curves near the crossing point is fairly mild may contribute to explain the existence of a wide region suitable for tree-grass coexistence at average rainfall rates. The pronounced interannual variability of both rainfall parameters might further enhance the possibility of coexistence by randomly driving the ecosystem from an increase in grasses during dry years to tree encroachment during wet years. A similar mechanism has been found to be a possible reason for tree-grass coexistence in the savannas of southern Texas, where a strong interannual rainfall variability induces marked fluctuations in the percentage of tree canopy coverage [cf. *Archer et al.*, 1988; *Rodriguez-Iturbe et al.*, 1999b; *Laio et al.*, 2001b].

[36] A comparison of Figures 7 and 8 reveals that the region of similar water stress is also the region where the difference in rooting depth is less important in controlling the water balance. This agrees with what is reported for the Nylsvley savanna, where the rainfall regime is similar to that of the central part of the Kalahari transect ($\lambda = 0.17\ d^{-1}$, $\alpha = 1.5$ cm) and both trees and grasses have a consistent root density up to the depth of one meter [*Scholes and Walker*, 1993; *Laio et al.*, 2001b].

[37] **Acknowledgments.** The authors gratefully acknowledge the support of NASA through the grant NAG5-9357 and of NSF through the grant DEB-0083566. K.K. Caylor was also supported by a NASA Earth System Science Fellowship.

References

Annegarn, H. J., S. Cole, L. T. Suttles, and R. Swap, SAFARI 2000 dry-season airborne campaign, *Earth Obs.*, *12*(5), 18–22, 2001.

Archer, S., C. Scifres, C. R. Bassham, and R. Maggio, Autogenic succession in a subtropical savanna: Conversion of grassland to thorn woodland, *Ecol. Monogr.*, *58*, 90–102, 1988.

Clapp, R. B., and G. N. Hornberger, Empirical equations for some soil hydraulic properties, *Water Resour. Res.*, *14*(8), 601–604, 1978.

Dowty, P., et al., Summary of the SAFARI 2000 wet season field campaign along the Kalahari transect, *Earth Obs.*, *12*(3), 29–34, 2001.

Dunne, T., Field studies of hillslope flow processes, in *Hillslope Hydrology*, edited by M. J. Kirkby, pp. 227–293, John Wiley, New York, 1978.

Laio, F., A. Porporato, L. Ridolfi, and I. Rodriguez-Iturbe, Plants in water-controlled ecosystems: Active role in hydrological processes and response to water stress, II, Probabilistic soil moisture dynamics, *Adv. Water Res.*, *24*(7), 707–723, 2001a.

Laio, F., A. Porporato, C. P. Fernandez-Illescas, and I. Rodriguez-Iturbe, Plants in water-controlled ecosystems: Active role in hydrological processes and response to water stress, IV, Discussion of real cases, *Adv. Water Res.*, *24*(7), 745–762, 2001b.

Pike, J. G., The development of the water resources of the Okavango Delta, in *Proceedings of the Conference on Sustained Production for Semi-Arid Areas*, *Botswana Notes and Records*, spec. ed. 1, pp. 35–40, Botswana Soc., Gabarone, Botswana, 1971.

Porporato, A., F. Laio, L. Ridolfi, and I. Rodriguez-Iturbe, Plants in water-controlled ecosystems: Active role in hydrological processes and response to water stress, III, Vegetation water stress, *Adv. Water Res.*, *24*(7), 725–744, 2001.

Rodriguez-Iturbe, I., A. Porporato, L. Ridolfi, V. Isham, and D. Cox, Probabilistic modeling of water balance at a point: The role of climate, soil and vegetation, *Proc. R. Soc. London Ser. A*, *455*, 3789–3805, 1999a.

Rodriguez-Iturbe, I., P. D'Odorico, A. Porporato, and L. Ridolfi, Tree-grass coexistence in savannas: The role of spatial dynamics and climate fluctuations, *Geophys. Res. Lett.*, *26*(2), 247–250, 1999b.

Scholes, R. J., and D. A. B. Parsons (Eds.), *The Kalahari Transect: Research on Global Change and Sustainable Development in South Africa*, *IGBP Rep. 42*, Stockholm, Int. Geosphere-Biosphere Prog. Secr., Stockholm, 61 pp., 1997.

Scholes, R. J., and B. H. Walker, *An African Savanna*, Cambridge Univ. Press, New York, 1993.

Scholes, R. J., P. R. Dowty, K. Caylor, D. A. B. Parsons, P. G. H. Frost, and H. H. Shugart, Trends in savanna structure and composition on an aridity gradient in the Kalahari, *J. Veg. Sci.*, *13*(3), 419–428, 2002.

Swap, R., J. T. Suttles, H. Annegarn, Y. Scorgie, J. Closs, J. Privette, and B. Cook, Report on SAFARI 2000 outreach activities, intensive field campaign planning meeting, and data management workshop, *Earth Obs.*, *12*(3), 26–28, 2001.

Thomas, D. S. G., and P. A. Shaw, *The Kalahari Environment*, Cambridge Univ. Press, New York, 1991.

Tyson, P. D., *Climatic Change and Variability in Southern Africa*, Oxford Univ. Press, New York, 1986.

Tyson, P. D., and S. J. Crimp, The climate of the Kalahari transect, *Trans. R. Soc. S. Afr.*, *53*, 93–112, 1998.

K. K. Caylor, Department of Environment Sciences, University of Virginia, Charlottesville, VA, USA.

A. Porporato, F. Laio, and L. Ridolfi, Dipartimento di Idraulica Trasporti ed Infrastrutture Civili, Politecnico di Torino, Corso Duca degli Abruzzi 24, I-10129, Torino, Italy. (porporato@polito.it)

I. Rodriguez-Iturbe, Department of Civil and Environmental Engineering and Center for Energy and Environmental Studies, Princeton University, Princeton, NJ, USA.